How a Flow Aligned Mesh Improves TELEMAC Model Results

Sven Smolders
sven.smolders@mow.vlaanderen.be, Antwerp, Belgium
Flanders Hydraulics Research, dept. of Mobility and Public Works, Flemish Government

Abstract –**In an unstructured 2D mesh the quality can be checked by means of checking the aspect ratio of the individual triangles or even the edge growth ratio. This paper wants to show how the orientation of the triangles can also affect the model results. An estimation of the longitudinal and lateral numerical diffusion is given explaining why flow alignment can be beneficial in reducing the numerical diffusion. This is demonstrated for the advection of a tracer with the rotating cone example.**

The paper also shows an example of a 3D hydrodynamic model of the Scheldt estuary. A comparison is made between a good quality mesh and a flow aligned mesh for the same model domain. All variables are kept equal. The influence on tidal propagation is shown. The effect on the bottom friction coefficient is shown and the potential effect on a coupled sediment transport model is discussed.

The flow aligned mesh reduces the amount of lateral numerical diffusion, it reduces the artificial loss of tidal energy along the estuary, and it improves the calibration result by getting more realistic bottom friction coefficients.

Keywords: Flow aligned mesh, numerical diffusion, advection scheme, rotating cone.

I. INTRODUCTION

At Flanders Hydraulics Research, several Scheldt Estuary models exist in different software packages ranging from a 1D DHI Mike11 model [1], over a TELEMAC-2D model [2], to a TELEMAC-3D model [3] and a Delft3D Simona model [4]. All these models were calibrated using a varying Manning bottom friction coefficient. Water levels measured at different tide gauges were compared with modeled water levels. The spatial varying bottom friction coefficient between each two tide gauges is used to calibrate the water levels in these models. If a modeled water level is higher than the measured value, the bottom friction coefficient is increased and vice versa. In this way the bottom friction coefficient is used as the one parameter to correct for all physical (e.g. bad representation of bathymetry by the mesh or a too simplistic turbulence model) and non-physical (e.g. diffusive advection scheme) errors in the model.

All the forementioned models use a Manning coefficient for the bottom friction and all models were calibrated according to the same method (spatially varying bottom friction coefficient) described above. When calibrating the TELEMAC models it was noticed that, in the upstream part of the estuary, very low Manning coefficients were necessary to correct the water levels. Lowering the Manning coefficient even more was no longer helping to correct the water levels properly. When the Manning coefficients of the four models were compared to each other, see Figure 1, it can be seen that both the 1D Mike 11 model as the Delft3D model have much higher Manning coefficients upstream the estuary.

The same problem was reported in [5] where a TELEMAC-2D model of a tributary of the Weser estuary was presented. Lowering the bottom friction coefficient could not further improve modeled water levels either. Numerical diffusion generated by the advection schemes was pointed out as the problem.

For the TELEMAC-3D Scheldt estuary model the non-physical Manning bottom friction coefficients and the generated numerical diffusion resulted also in problems in the coupled sediment model. A different (physical realistic) bottom friction coefficient needed to be programmed in the code. The very diffusive upstream part of the estuary also did not solve well the cohesive sediment transport. It is known that numerical diffusion decreases, and solver accuracy increases, with a higher resolution mesh and better quality of the triangles used, i.e. triangles must be as equilateral as possible. This was however already the case for this detailed TELEMAC-3D Scheldt estuary model [3].

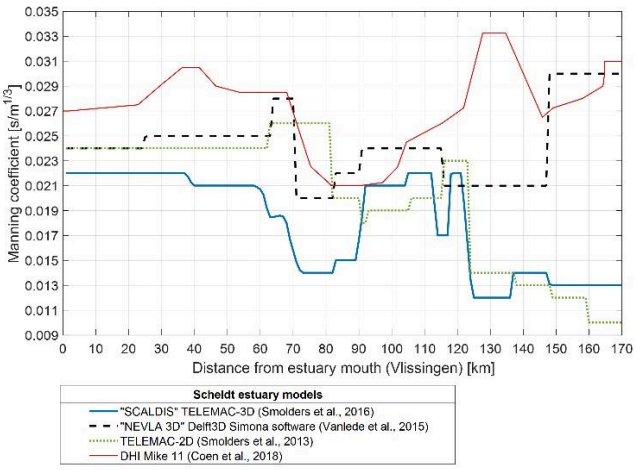

Figure 1. Manning bottom roughness coefficient along the Scheldt estuary for different kind of models

This paper wants to show that besides the mesh quality in terms of triangle shape, proper alignment of the triangles to flow direction or structures can have a large impact on the quality of the model results. the effect of mesh quality, i.e. proper mesh alignment to be precise, on the results of a TELEMAC simulation.

First some general information about grid diffusion and mesh alignment is given. Next the effect of a better flow aligned mesh is demonstrated with an example of tracer advection with a rotating cone. This simple example shows the effect of mesh alignment on numerical diffusion caused by

different advection schemes. Finally, the results of a new flow aligned mesh for the TELEMAC-3D Scheldt estuary model are shown. The Manning bottom friction coefficients before and after mesh alignment will be shown.

II. GRID DIFFUSION AND MESH ALIGNMENT

In [6], an analytical derivation and estimation of grid diffusion is given for a 2D finite element model of the Francisco Bay estuary. The authors start from the modified equation analysis normally applied on finite difference grids [7] and a 1-D, first-order, forward-in-time, backward-in-space scalar advection scheme. The difficulty for applying this on an unstructured grid is that half of the elements have one inflow face and two outflow faces (type B element in Figure 2), and the other half have two inflow faces and one outflow face (type A element in Figure 2). In this paper only the outcome of the derivation in [6] is given in the form of an expression for the longitudinal numerical diffusion coefficient (along the x-axis), K^x (1), the lateral diffusion coefficient (along the y-axis), K^y (2), and the cross-diffusion coefficient, K^{xy} (3). Some assumptions were made: the scalar values are cell averages and are located at the circumcentre of each element. The mesh consists only of equilateral triangles and the angle, θ, gives the orientation of the grid relative to the x-axis (Figure 2). The free-stream velocity U is taken parallel to the x-axis and the edge length of an element is denoted by l (Figure 2). The cross term only gives information about the orientation of diffusion whereas the magnitude of the numerical diffusion depends only on K^x and K^y.

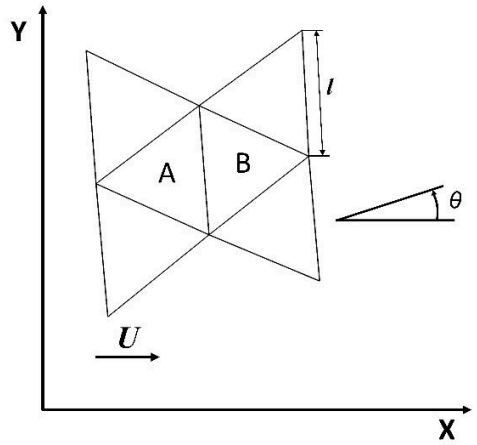

Figure 2. Schematic representation of a mesh with equilateral triangles in a cartesian coordinate system with an overall flow velocity U along the X-axis and θ the angle between a triangle's edge and the X-axis (after [6]).

In a flow aligned mesh (Figure 3) the lateral numerical diffusion equals to zero for $\theta = 0$ (2), because of the averaging over two consecutive type A and type B elements. Any diffusive spreading is geometrically limited to a single width triangle strip as the flow aligned faces have zero flux.

$$K^x = \left[\frac{2\sqrt{3}}{3}\left(cos^2\theta \cos\left(\theta+\frac{\pi}{6}\right) + sin\theta\, cos^2\left(\theta-\frac{\pi}{3}\right)\right) - \frac{\sqrt{3}}{4\sin\left(\theta+\frac{\pi}{3}\right)}\right]\frac{Ul}{2} - \frac{U^2\Delta t}{2} \quad (1)$$

$$K^y = \frac{\sin(3\theta)}{4\sqrt{3}}Ul \quad (2)$$

$$K^{xy} = \left[\frac{2}{\sqrt{3}}sin\theta \sin\left(\theta-\frac{\pi}{6}\right)\sin\left(\theta-\frac{\pi}{3}\right)\right]Ul \quad (3)$$

For a flow aligned grid, when $\theta = 0$, the longitudinal numerical diffusion simplifies to

$$K^x = \frac{Ul}{4} - \frac{U^2\Delta t}{2} \quad (4)$$

Equations (1-3) quantify how much the orientation of the mesh elements affects numerical diffusion and show that elements aligned with the velocity field have no lateral numerical diffusion. This shows that for models where sections of the flow have a dominant direction, it is worthwhile to create a flow aligned section of mesh. In these sections triangles do not even need to be equilateral. Because of the no-flux faces, triangles can be stretched in the dominant flow direction without too much consequences for the quality of the results.

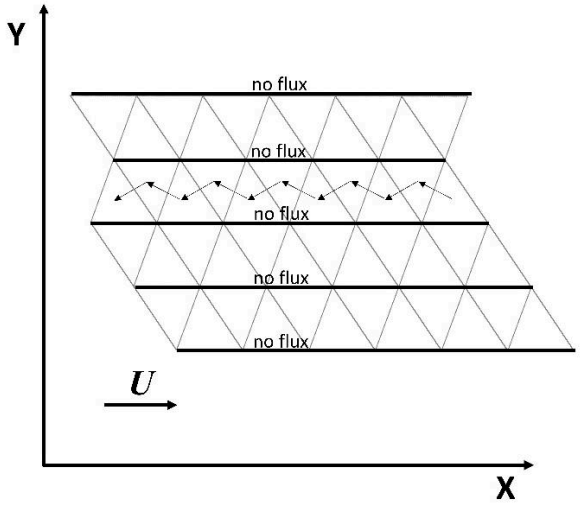

Figure 3. Schematic flow aligned mesh showing no lateral diffusion because of the zero-flux faces. The arrows show the flux for each individual element evaluated for each element's upwind neighbour (after [6]).

III. ROTATING CONE

A. test case for advection of tracer

The rotating cone test case is described in the TELEMAC validation document in 2D in [8] and 3D in [9]. It shows the effect of the different finite element advection schemes on the passive scalar transport. This test case shows the advection of a tracer in a square basin with a flat frictionless bottom and closed boundaries. The dimensions are 20 x 20 m and the mesh is a regular grid where all squares were cut in half (see left panel in Figure 4). The mesh contains 441 nodes and 800 elements. The water depth is constant in time and equal to 2 m. The rotating velocity field is also constant in time and free of divergence. The angular velocity is set to 1 rad.s^{-1} which gives a rotation period of T=2π (6.28 s). The centre of the mesh is the centre of the rotation (x_0=10 m and y_0= 10 m). The initial value for the tracer is given by a Gaussian function off-centered 5 m to the right of (x_0, y_0) representing a cone. The tracer diffusivity is set to zero. In both [8] as [9] are 1D solutions along a slice plane (x, y), y=10 m after a half and a full rotation given to

show which advection schemes preserve the tracer cone the best. In [8] is also shown how an increase in mesh resolution decreases the error propagating on the mesh in the results, i.e. a higher resolution results in less numerical diffusion. The increased resolution demanded in some cases also for a decrease in time step to keep a stable Courant criterium (5) close to unity.

$$C = \frac{u*\Delta t}{\Delta x} \leq C_{max} \quad (5)$$

where C represents the dimensionless Courant number, u is the magnitude of the flow velocity, Δt is the time step, Δx is the mesh resolution, and C_{max} depends on the solver method (where for an explicit solver this value should be close to 1 for stability).

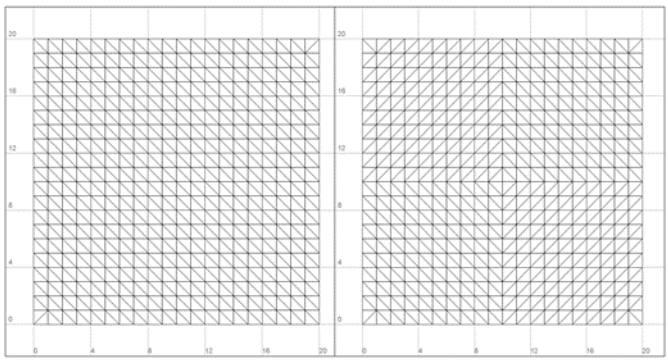

Figure 4. Rotating cone mesh original (left) and simple change for better flow alignement (right)

B. *simple change in mesh to make it more flow aligned*

In the upper left and lower right quadrant of the mesh, the longest edge of the triangles was rotated 90 degrees, resulting in the mesh given in Figure 4 on the right. This makes the mesh more flow aligned with the rotating velocity field. Note that this mesh is still very coarse and that this mesh needs refinement for proper flow alignment. But the current simple intervention in the mesh will show how tracer advection is impacted and will show the potential for further decrease in numerical diffusion.

C. *Difference in advection of tracers*

Like in [8] and [9] the 1D solution along a slice plane (x, y), y=10 m after a half (Figure 5) and a full rotation (Figure 6) are given here with the results for the original mesh in dashed lines (including the analytical solution) and the results for the adjusted and more flow aligned mesh in full line. To keep both figures uncluttered only the results of advection schemes Weak characteristics (blue), NERD (green) and LIPS (yellow) are shown.

Even though the mesh in the example is coarse and the changes made to make it more flow aligned were minimal, the results clearly show a decrease in the numerical diffusion generated by the different advection schemes. For the Weak Characteristic scheme the results are not that different, but this scheme already performs well and generates the least amount of numerical diffusion of all schemes.

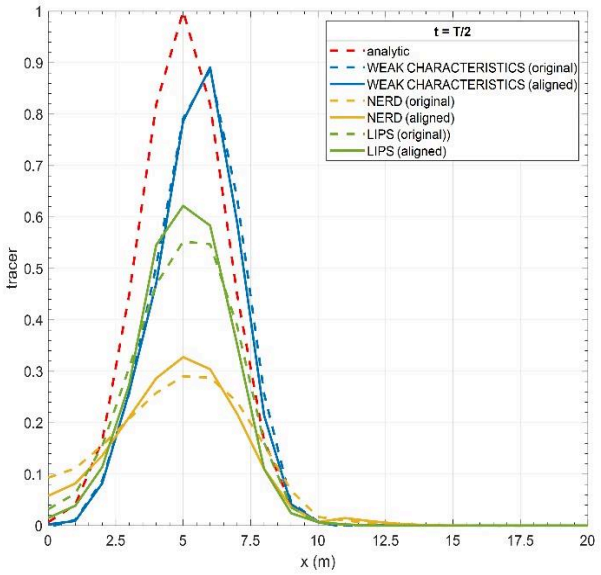

Figure 5. Rotating cone results after a half rotation (t = T/2) for original mesh (dashed lines) and the flow aligned mesh (solid lines) for the Weak Characteristics (blue), NERD (green) and LIPS (yellow) advection schemes. The analytical solution is given in dashed red line.

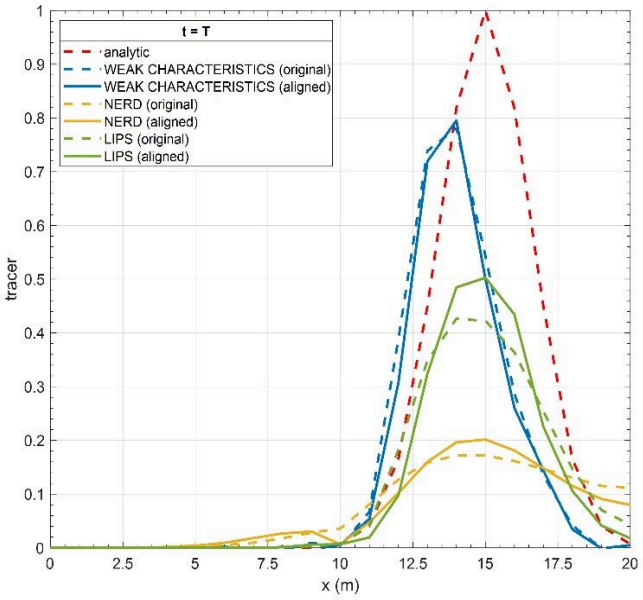

Figure 6. Rotating cone results after one rotation (t = T) for original mesh (dashed lines) and the flow aligned mesh (solid lines) for the Weak Characteristics (blue), NERD (green) and LIPS (yellow) advection schemes. The analytical solution is given in dashed red line.

IV. SCHELDT ESTUARY APPLICATION

A. Flow aligned mesh

For the TELEMAC-3D Scheldt estuary model a new mesh was made using flow lines and a channel mesher to create a mesh that is more flow aligned. Even for the downstream part, which has multiple channels over its width, the mesh was flow aligned inside these channels. In the upstream parts, characterised by a single channel, the channel mesher was used to create more flow aligned structured unstructured mesh. In some parts where the flow direction was really unidirectional, the triangles were even stretched in the flow direction.

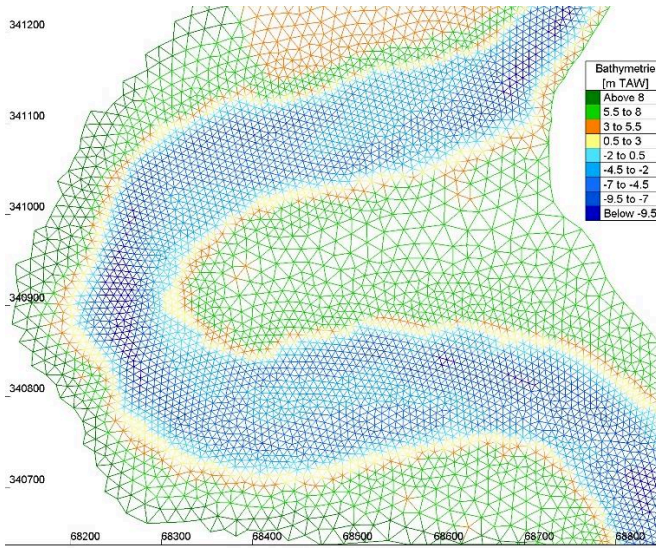

Figure 7. Detail of the mesh at the sharpest bend in the upstream part (km 143-146) of the Scheldt estuary in the original TELEMAC-3D model mesh.

A detail of the original mesh is shown in Figure 7. It shows that the original mesh already contained sufficient mesh resolution to well represent the bathymetry. It also shows that most of the triangles meet the mesh quality standard of being as much equilateral as possible. Figure 8 shows the same location but in the flow aligned mesh. The Blue Kenue Channel mesher was used here and triangles were stretched a little in the longitudinal direction. Although the mesh resolution in this section is coarser for the flow aligned mesh, the overall node count for both meshes was in the same order of around 290000 nodes in 2D.

B. Results

For both simulations all parameters were kept as in the original model [3]and only the mesh changed. So both simulation were performed with the spatially varying bottom friction coefficients of the original calibrated TELEMAC-3D Scheldt estuary model [3]. Figure 9 shows the maximum water level along the estuary for an average tide. From the mouth to upstream the difference in water level keeps increasing along the estuary showing higher water levels for the simulation with the flow aligned mesh.

In a second step the model with the flow aligned mesh was calibrated so that water levels would coincide with the original model. The Manning bottom friction coefficient was used and varied spatially like the original model. The result is shown in Figure 10. The Manning bottom friction coefficient in the flow aligned mesh version is higher than in the original version. In the upstream part the flow aligned version can keep the Manning coefficient at a decent physical level showing a significant reduction in numerical diffusion of the tidal energy in this upper part.

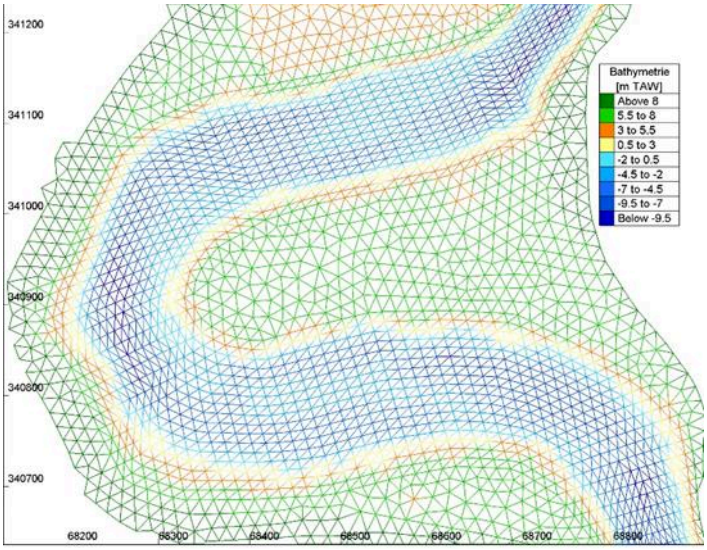

Figure 8. Detail of the mesh at the sharpest bend in the upstream part (km 143-146) of the Scheldt estuary in the flow aligned mesh version of the TELEMAC-3D model

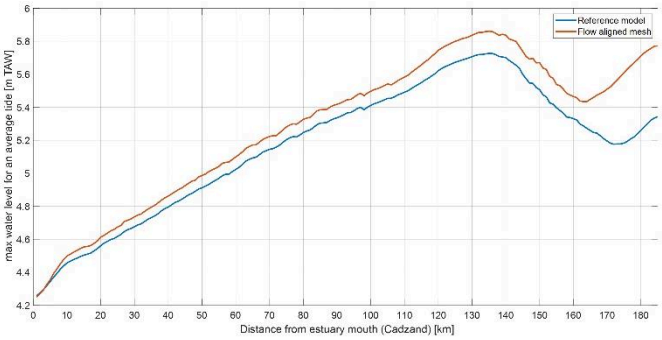

Figure 9. Maximum water level comparison along the Scheldt estuary model results for the original TELEMAC-3D Scheldt estuary model and the new flow aligned mesh. Both simulations used the original calibrated spatially varying bottom friction coefficients.

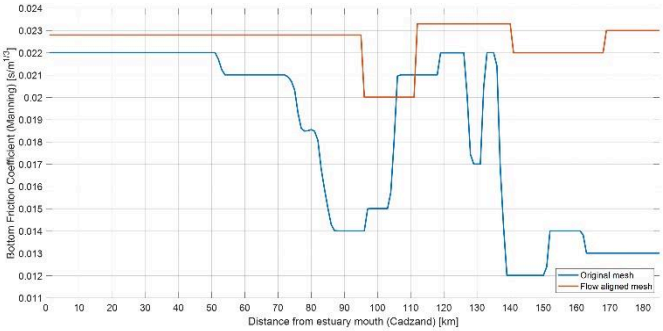

Figure 10. Manning bottom roughness coefficient for the original TELEMAC-3D model (blue line) and for the flow aligned mesh version (orange line)

C. *discussion*

A high quality and good designed structured unstructured mesh can possess faces which are either tangent or normal to the flow field. Construction of flow aligned meshes require more work and a better understanding of the model domain. Higher accuracy and less numerical dissipation can be achieved. Flow alignment of the mesh in region with a dominant flow direction allows for more effective application of solvers in the flux computations, leading to a reduction in discretisation error. The mesh locally mimics the attributes of a structured grid and provides high quality numerical solutions due to the alignment of the element interfaces.

Energy is dissipated by three mechanisms: turbulence, bottom friction and numerical diffusion. In this example by flow aligning the mesh the numerical diffusion was decreased (which probably also affected turbulent dispersion) and therefore the Manning bottom friction coefficient could be increased to reach again physical meaningful values.

D. *Coupled cohesive sediment transport model*

When coupling a sediment transport model, the quality of the hydrodynamic model determines the maximum quality of the sediment transport model. By applying the flow aligned mesh and retrieving again realistic Manning coefficient values for the upstream part of the estuary, the coupled sediment model can use them directly from the hydrodynamic simulation.

One of the problems in the (cohesive) sediment transport model [10] is the large amount of sediments that ended up on the tidal flats, especially in the upstream part of the estuary. The increase in Manning coefficient and the better representation of the tidal velocities in the flow aligned model will increase the local bed shear stress and resuspend more sediment than before.

Furthermore, according to [11] the longitudinal diffusion coefficient K^x is inversely proportional to the lateral one K^y (6).

$$K^x \sim \frac{U^2 h^2}{K^y} \quad (6)$$

with h the water depth. With K^y smaller or close to zero implies an inefficient lateral mixing which tends to increase the effect of differential advection which in turn will improve sediment transport.

Further testing is needed to see if the above-mentioned improvements really improve the sediment transport model.

V. CONCLUSION

In the CFD world mesh alignment to flow features is well known and part of the quality concept of the mesh. In the world of TELEMAC hydrodynamics it is less known and it is hoped that this paper demonstrates the potential for model result improvement for model domains that have dominant one-directional flow fields. It is certainly suited for estuarine applications and especially in the upstream parts where bottom friction is already a dominant tidal energy dissipator. No need to add artificial energy dissipation to the equation.

ACKNOWLEDGEMENT

I would like to thank Kai Chu from IMDC and my colleague Qilong Bi for some interesting discussions on this topic and helping me reach a next step in the quality of our TELEMAC models.

REFERENCES

[1] Coen, L.; Deschamps, M.; Vanderkimpen, P.; Mostaert, F. (2018). Mike11 model Zeeschelde en tijgebonden zijrivieren: Beschrijving versie 2015. Versie 4.0. WL Rapporten, 14_106_6. Waterbouwkundig Laboratorium: Antwerpen.

[2] Smolders, S., Meire, P., Temmerman, S., Cozzoli, F., Ides, S., & Plancke, Y. M. (2013). A 2Dh hydrodynamic model of the Scheldt estuary in 1955 to assess the ecological past of the estuary. In XXth TELEMAC-MASCARET. User Conference 2013 (pp. 137-143).

[3] Smolders, S.; Maximova, T.; Vanlede, J.; Plancke, Y.; Verwaest, T.; Mostaert, F. (2016). Integraal plan Bovenzeeschelde: Subreport 1. SCALDIS: a 3D Hydrodynamic model for the Scheldt Estuary. WL Rapporten, 13_131. Flanders Hydraulics Research: Antwerp

[4] Vanlede, J.; Delecluyse, K.; Primo, B.; Verheyen, B.; Leyssen, G.; Plancke, Y.; Verwaest, T.; Mostaert, F. (2015). Verbetering randvoorwaardenmodel: Subreport 7 - Calibration of NEVLA 3D. Version 4.0. WL Rapporten, 00_018. Flanders Hydraulics Research & IMDC: Antwerp, Belgium.

[5] Malcherek, A. (2000). Application of TELEMAC-2D in a narrow estuarine tributary. Hydrological processes, 14(13), 2293-2300.

[6] Holleman, R., Fringer, O., & Stacey, M. (2013). Numerical diffusion for flow-aligned unstructured grids with application to estuarine modeling. International Journal for Numerical Methods in Fluids, 72(11), 1117-1145.

[7] Warming R, Hyett B. The modified equation approach to the stability and accuracy analysis of finite-difference methods. Journal of Computational Physics 1974; 14(2):159–179.

[8] TELEMAC-2D Validation Manual Version v8p3, chapter 13 Advection of tracers with a rotating cone. December 6, 2021.

[9] TELEMAC-3D Validation Manual Version v8p3, chapter 14 Advection of tracers with a rotating cone. December 6, 2021.

[10] Smolders, S.; Bi, Q.; Vanlede, J.; De Maerschalck, B.; Plancke, Y.; Mostaert, F. (2020). Integraal plan Boven-Zeeschelde: Sub report 6 – Scaldis Mud: a Mud Transport model for the Scheldt Estuary. Version 4.0. FHR Reports, 13_131_6. Flanders Hydraulics Research: Antwerp.

[11] Fischer HB, List EJ, Koh RC, Imberger J, Brooks NH. Mixing in Inland and Coastal Waters. Academic Press, Inc.: New York, 1979.